Roles of Aromatic Residues in High Interfacial Activity of *Naja naja atra* Phospholipase A_2[†]

Marius Sumandea,[‡] Sudipto Das,[‡] Claudia Sumandea, and Wonhwa Cho*

Department of Chemistry (M/C 111), University of Illinois at Chicago, 845 West Taylor Street, Chicago, Illinois 60607-7061

Received September 14, 1999; Revised Manuscript Received October 5, 1999

ABSTRACT: Acidic phospholipase A_2 (PLA_2) from the venom of Chinese cobra (*Naja naja atra*) has high activity on zwitterionic membranes and contains six aromatic residues, including Tyr-3, Trp-18, Trp-19, Trp-61, Phe-64, and Tyr-110, on its putative interfacial binding surface. To assess the roles of these aromatic residues in the interfacial catalysis of *N. n. atra* PLA_2, we mutated them to Ala and measured the effects on its interfacial catalysis. Enzymatic activities of the mutants toward various vesicle substrates and human neutrophils indicate that all but Trp-18 make significant contributions to interfacial catalysis. Among these aromatic residues, Trp-19, Trp-61, and Phe-64 play the most important roles. Binding affinities of the mutants for phospholipid-coated beads and their monolayer penetration indicate that Trp-19, Trp-61, and Phe-64 are critically involved in interfacial binding of *N. n. atra* PLA_2 and penetrate into the membrane during the interfacial catalysis of *N. n. atra* PLA_2. Further thermodynamic analysis suggests that the side chain of Phe-64 is fully inserted into the hydrophobic core of membrane whereas those of Trp-19 and Trp-61 are located in the membrane−water interface. Together, these results show that all three types of aromatic residues can play important roles in interfacial binding of PLA_2 depending on their location and side-chain orientation. They also indicate that these aromatic side chains interact with membranes in distinct modes because of their different intrinsic preference for different parts of membranes.

Phospholipases A_2 (PLA_2;[1] E.C. 3.1.1.4) catalyze the hydrolysis of the fatty acid ester in the 2-position of 3-*sn*-phospholipids and are found both in intracellular and secreted forms. Secretory PLA_2s are small proteins (13−15 kDa) that can be classified into at least five groups on the basis of differences in primary structure (*1*). Crystallographic and NMR analyses of multiple secretory PLA_2s have shown that they have similar overall tertiary structural folds (*2*). Despite their structural similarity, secretory PLA_2s show a wide rage of enzymatic and pharmacological activities. Most secretory PLA_2s have high activity toward anionic membranes due in part to the presence of cationic residues on their interfacial binding surface (*3*−*6*). However, they show significantly lower activity on zwitterionic membranes, such as phosphatidylcholine (PC) vesicles and intact mammalian cells whose outer plasma membrane is composed mainly of zwitterionic PC and sphingomyelin. Only a small number of PLA_2s, most notably some PLA_2s from cobra venom, show high activity toward PC vesicles and intact mammalian cell membranes. We (*7, 8*) and others (*9*) have recently shown that the presence of a single tryptophan residue on the interfacial binding surface of PLA_2 can dramatically enhance its activity toward zwitterionic membranes. A major acidic PLA_2 from the venom of Chinese cobra (*Naja naja atra*) is highly active on zwitterionic membranes and contains a number of aromatic residues, including three tryptophans, on its putative interfacial binding surface (*10*). In this study, we performed a structure−function analysis of the *N. n. atra* PLA_2 to quantitatively assess the contributions of the aromatic residues to its high activity on PC membranes. Herein, we describe the enzymatic activities, binding affinities, and monolayer penetration behaviors of selected mutants, which indicates that most of the surface aromatic residues significantly contribute to interfacial binding but interact with membranes in different modes.

MATERIALS AND METHODS

Materials. 1-Hexadecanoyl-2-(1-pyrenyldecanoyl)-*sn*-glycero-3-phosphoethanolamine (pyrene-PE) and -glycerol (pyrene-PG) were purchased from Molecular Probes (Eugene, OR). 1,2-Di-*O*-hexadecyl-*sn*-glycero-3-phosphocholine (DHPC) was purchased from Sigma. [^{3}H]Arachidonic acid was from American Radiochemical Co. (St. Louis, MO). All commercial lipids were used without further purification. 1,2-Di-*O*-hexadecyl-*sn*-glycero-3-phosphoglycerol (DHPG) was prepared from DHPC by phospholipase D-catalyzed transphosphatidylation as described by Comfurius and Zwaal (*11*).

1,2-Bis[12-(lipoyloxy)dodecanoyl]-*sn*-glycero-3-phosphoglycerol (BLPG) was prepared as described elsewhere (*12*,

[†] This work was supported by NIH grants (GM53987 and GM52598) and a Biomedical Science Grant from the Arthritis Foundation. W.C. is an Established Investigator of the American Heart Association.

* To whom correspondence should be addressed: Tel 312-996-4883; FAX 312-996-2183; E-mail wcho@uic.edu.

[‡] These authors equally contributed to this work.

[1] Abbreviations: BLPC, 1,2-bis[12-(lipoyloxy)dodecanoyl]-*sn*-glycero-3-phosphocholine; BLPG, 1,2-bis[12-(lipoyloxy)dodecanoyl]-*sn*-glycero-3-phosphoglycerol; BSA, bovine serum albumin; DHPC, 1,2-di-*O*-hexadecyl-*sn*-glycero-3-phosphocholine; DHPG, 1,2-di-*O*-hexadecyl-*sn*-glycero-3-phosphoglycerol; EDTA, ethylenediaminetetraacetate; HBSS, Hanks' balanced salt solution; PC, phosphatidylcholine; PG, phosphatidylglycerol; PLA_2, phospholipase A_2; pyrene-PE, 1-hexadecanoyl-2-(1-pyrenyldecanoyl)-*sn*-glycero-3-phosphoethanolamine; pyrene-PG, 1-hexadecanoyl-2-(1-pyrenyldecanoyl)-*sn*-glycero-3-phosphoglycerol; SDS, sodium dodecyl sulfate.

10.1021/bi9921384 CCC: $18.00
Published on Web 11/16/1999

13). Phospholipid concentrations were determined by phosphate analysis (*14*). Styrene−divinylbenzene beads (5.2 ± 0.3 μm diameter) were purchased from Seradyn (Indianapolis, IN). Fatty acid-free bovine serum albumin (BSA) was from Bayer Inc. (Kankakee, IL). 5,5′-Dithiobis(2-nitrobenzoic acid) and sodium sulfite were obtained from Aldrich. 2-Nitro-5-(sulfothio)benzoate was synthesized from 5,5′-dithiobis(2-nitrobenzoic acid) as described by Thannhauser et al. (*15*). Oligonucleotides were purchased from Integrated DNA Technologies (Coralville, IA) and further purified on polyacrylamide gels. Restriction endonucleases and other enzymes for molecular biology were obtained from either Boehringer Mannheim or New England Biolabs (Beverly, MA). Ampicillin, sodium deoxycholate, phenylmethanesulfonyl fluoride, urea, and guanidinium chloride were from Sigma. Triton X-100 was purchased from Pierce.

Construction of N. n. atra PLA_2 Expression Vector. Synthetic *N. n. atra* PLA_2 gene (see Figure 1) containing an Asn to Gly mutation at the amino terminus was constructed by the strategy used previously (*16*, *17*). Two DNA fragments containing 200 base pairs (fragment 1) and 212 base pairs (fragment 2), respectively, were designed with two unique restriction sites at the 5′ and 3′ ends: *Nde*I and *Bgl*II for fragment 1 and *Bgl*II and *Hin*dIII for fragment 2. Each gene fragment was prepared from four partially overlapping single-stranded oligonucleotides (64−71 bases long) whose complementary regions were about 20 bases long. Oligonucleotides used were as follows: oligo-1 (69-mer), 5′-GGA GTA CCT CAT ATG GGC CTG TAC CAG TTC AAA AAC ATG ATC CAG TGC ACC GTT CCG TCT CGT TCT TGG-3′; oligo-2 (64-mer), 5′-GAA CCA CCA CGA CCG CAG TAG CAA CCG TAG TCA GCG AAG TCC CAC CAA GAA CGA GAC GGA ACG G-3′; oligo-3 (66-mer), 5′-GCT ACT GCG GTC GTG GTG GTT CTG GTA CCC CGG TTG ACG ACC TGG ACC GTT GCT GCC AGG TTC ACG-3′; oligo-4 (63-mer), 5′-GGC CAA CAA CCA GAG ATC TTT TCA GCT TCG TTG TAG CAG TTG TCG TGA ACC TGG CAG CAA CGG-3′; oligo-5 (69-mer), 5′-GCT GAA AAG ATC TCT GGT TGT TGG CCG TAC TTC AAA ACC TAC TCT TAC GAA TGC TCT CAG GGT ACT CTG-3′; oligo-6 (70-mer) 5′-GCA ATC GCA AAC AGC AGC TGC ACA TGC GTT GTT ACC ACC TTT GCA GGT CAG AGT ACC CTG AGA GCA TTC G-3′; oligo-7 (68-mer) 5′-CAG CTG CTG TTT GCG ATT GCG ATC GTC TGG CTG CAA TCT GCT TCG CTG GTG CTC CGT ACA ACA ACA AC-3′; oligo-8 (71-mer), 5′-GGT GGA AGC TTA CTA CTG GCA ACG AGC TTT CAG GTC GAT GTT GTA GTT GTT GTT GTT GTA CGG AGC ACC AG-3′. To obtain each double-stranded gene fragment, the respective four oligonucleotides (1 μg each) were mixed, annealed, and extended with T7 DNA polymerase (0.8 unit) or Klenow DNA polymerase (4 units) for 30 min. The products were analyzed on 2% agarose gels and the major band for each fragment was excised, purified, and amplified by polymerase chain reaction with *Pfu* DNA Polymerase (Stratagene, La Jolla, CA) and two flanking primers (oligo-1 and -4 for fragment 1 and oligo-5 and -8 for fragment 2). The polymerase chain reaction consisted of 25 cycles of 95 °C for 1 min, 55 °C for 2 min, and 72 °C for 1 min. The products were separated on 2% agarose gels and the major band for each fragment was excised and purified with a QIAquick gel extraction kit (Qiagen, Valencia, CA). Then, the fragments 1 and 2 were digested with *Nde*I/*Bgl*II and *Bgl*II/*Hin*dIII, respectively, and subcloned into pET21d vector (Novagen, Madison, WI) to yield plasmid I and plasmid II, which were then transformed into JM109 cells for amplification. Finally, fragment 1 was separated from plasmid I digested by *Nde*I/*Bgl*II and subcloned into the *Nde*I/*Bgl*II site of plasmid II to yield a complete expression vector for *N. n. atra* PLA_2 (pMS-nna). The nucleic acid sequence of the entire coding region of the plasmid was verified by sequencing analysis with a Sequenase 2.0 kit (Amersham-Pharmacia).

Site-Directed Mutagenesis. Specific mutations were introduced directly into the pMS-nna plasmid construct by using QuickChange site-directed mutagenesis kit (Stratagene) according to the manufacturer's instructions. Briefly, appropriate complementary synthetic oligonucleotides introducing desired mutations were used as primers for a polymerase chain reaction performed in a DNA thermal cycler (Perkin-Elmer) with *Pfu* DNA polymerase. Consequent transformation of *Dpn*I-treated linear double-stranded DNA into supercompetent *Epicurian coli* XL1-Blue cells (Stratagene) yielded clones, the identity of which was verified by DNA sequencing.

Expression and Purification of N. n. atra PLA_2. Escherichia coli strain BL21(DE3) was used as a host for protein expression. Two liters of Luria broth supplemented with 100 μg/mL ampicillin was inoculated with 1 mL of overnight culture from a single colony, grown at 37 °C. When the absorbance of the medium at 600 nm reached 0.2, additional ampicillin was added to a final concentration of 1 mM. Protein expression was induced with 1 mM isopropyl β-D-thiogalactopyranoside when the absorbance at 600 nm reached 0.8. After 4−5 h at 37 °C, cells were harvested at 3000*g* for 10 min at 4 °C and frozen at −20 °C overnight. Thawed cells were resuspended in 50 mL of 50 mM Tris-HCl buffer, pH 8.0, containing 2 mM ethylenediaminetetraacetate (EDTA), 50 mM NaCl, 1 mM phenylmethanesulfonyl fluoride, 0.4% (v/v) Triton X-100, and 0.4% (w/v) sodium deoxycholate and stirred at 4 °C. The suspension was sonicated on ice with a Sonifier 450 (Branson) in pulse mode for 15 × 15 s. The inclusion body pellet was obtained by centrifugation at 17000*g* for 20 min. The pellet was resuspended in 50 mL of 50 mM Tris-HCl buffer, pH 8.0, containing 2 mM EDTA, 50 mM NaCl, 1 mM phenylmethanesulfonyl fluoride, 0.8% (v/v) Triton X-100, and 0.8% (w/v) sodium deoxycholate, sonicated, and centrifuged as described above. The pellet was resuspended in 50 mL of the same buffer solution containing 1.2% (v/v) Triton X-100 and stirred for 30 min at room temperature. After centrifugation the inclusion bodies were washed with 50 mL of 50 mM Tris-HCl, pH 8.0, containing 5 M urea and 5 mM EDTA, and the suspension was centrifuged at 50000*g* and at 4 °C. The inclusion bodies were solubilized in 10 mL of 50 mM Tris-HCl, pH 8.5, containing 8 M guanidinium chloride and 0.3 M sodium sulfite, and stirred at room temperature for 30 min. Five milliliters of 2-nitro-5-(sulfothio)benzoate solution (50 mM) was then added, and the modification was completed in ca. 30 min. Any insoluble matter was removed by centrifugation at 100000*g* for 15 min at room temperature. The reaction mixture was loaded onto a Sephadex G-25 column (2.5 × 45 cm) equilibrated with 50 mM Tris-HCl buffer, pH 8.0, containing 5 M urea and 5

mM EDTA. The peak was collected (50 mL) at room temperature and dialyzed against water at 4 °C and then against 0.3% (v/v) glacial acetic acid to precipitate the sulfonated protein. The precipitated protein was resuspended in 100 mL of deionized water and the suspension was centrifuged at 17000*g* for 10 min at 4 °C. The protein pellet was then resuspended in 10 mL of 50 mM Tris-HCl buffer, pH 8.0, containing 5 mM EDTA and 5 M guanidinium chloride. To this solution of sulfonated protein, 40 mL of 50 mM Tris-HCl, pH 8.0, containing 40% (v/v) glycerol, 3% (w/v) sucrose, 5 mM EDTA, 20 mM reduced glutathione, and 10 mM oxidized glutathione was added dropwise with stirring (120 rpm) over 3−5 h. The solution was kept at room temperature for 20 h, at which point protein solution was dialyzed at 4 °C against 2 L of 25 mM Tris-HCl buffer containing 0.2 M guanidinium chloride and 10% (v/v) glycerol, pH 8.0, followed by 3 × 4 L of H_2O. The refolded protein solution was further purified on a HiLoad Q-Sepharose column (Amersham−Pharmacia). The purified PLA_2 was then dialyzed against distilled water and lyophilized. Native *N. n. atra* PLA_2 was purified from the lyophilized venom (Sigma) according to the procedure described for *Agkistrodon piscivorus piscivorus* PLA_2 (*18*). Protein purity was verified by SDS−polyacrylamide gel electrophoresis, and protein concentration was determined by the bicinchoninic acid method with BSA as standard (Pierce).

Kinetic Measurements. N. n. atra PLA_2-catalyzed hydrolysis of polymerized mixed liposomes was carried out at 37 °C in 2 mL of 10 mM Tris-HCl buffer, pH 7.4, containing 2.5 μM total phospholipids, 5 μM BSA, 0.16 M NaCl, and 10 mM $CaCl_2$ (*12, 13*). The progress of hydrolysis was monitored as an increase in fluorescence emission at 380 nm using a Hitachi F4500 fluorescence spectrometer with the excitation wavelength set at 345 nm. Spectral bandwidth was set at 10 nm for both excitation and emission. Values of $(k_{cat}/K_M)^*$ were determined from reaction progress curves as described previously (*5*).

Fatty Acid Release from Human Neutrophils. Human neutrophils were prepared from heparinized venous blood collected from medication-free donors. Briefly, 120 mL of whole blood was withdrawn from the antecubital vein and placed into containers containing 2 mL of 1:1000 heparin. Blood was diluted 1:1 with calcium-free Hanks' balanced salt solution (HBSS), layered over 15 mL of 1.089 g/mL Percoll, and centrifuged for 20 min at 900*g*. The supernatant and the mononuclear cells at the interface were aspirated carefully, and the inside wall of the tube was wiped with sterile gauze to remove mononuclear cells attached to the wall. To the pellet of neutrophils and erythrocytes was added 20 mL of ice-cold water, and the suspension was mixed gently for 30 s, after which 20 mL of 2× HBSS was added. If the erythrocytes remained, then the procedure was repeated. After the lysis of erythrocytes, neutrophils were washed once in HBSS/0.2% BSA, and the total cell count was determined with a Coulter counter. The resulting cell population consisted of >95% neutrophils. Radiolabeling of the cells was achieved by incubating the cells (10^7) with 0.5 Ci/mL [^{3}H]arachidonic acid for 90 min at 37 °C. Unincorporated [^{3}H]arachidonic acid was removed by washing the cells with HBSS/0.2% BSA. The cells were resuspended in HBSS/0.2% BSA (10^6 cells/90 μL) and incubated with 1 μM PLA_2 at 37 °C for 30 min. The reaction was quenched by centrifugation, and the supernatants were removed and their radioactivity was measured by liquid scintillation counting.

Binding of N. n. atra PLA_2 to Phospholipid-Coated Beads. To circumvent the complication due to low pelleting efficiency of PC vesicles, DHPC- and DHPG-coated styrene−divinylbenzene beads were used for measuring the interfacial binding affinity of *N. n. atra* PLA_2 (*19*). Phospholipid-coated beads were prepared as described previously (*19*). Phospholipid-coated beads were suspended in 2 mL of 10 mM Tris-HCl buffer, pH 7.4, containing 0.16 M NaCl and 10 mM $CaCl_2$. Final bulk phospholipid concentration was 200−300 μM. Aliquots (5−60 μL) of bead suspension were incubated at room temperature for 15 min in the same buffer (total volume, 150 μL) containing 1 μM BSA and varying concentrations of PLA_2. Under our binding assay conditions (i.e., in the presence of 1 μM BSA), nonspecific binding of protein to exposed hydrophobic surfaces of beads and tube walls is insignificant (*19, 20*). Mixtures were centrifuged for 5 min at 12000*g* and aliquots of the supernatants were assayed for PLA_2 activity using pyrene-PG/BLPG vesicles as substrates as described above. To preclude the possibility of protein aggregation and sedimentation during binding measurements, the binding mixtures minus phospholipid-coated beads were centrifuged and enzyme concentrations before and after centrifugation were compared. Values of n and K_d were determined by nonlinear least-squares analysis of the $[E]_b$ vs $[E]_0$ plot using

$$[E]_b = \{[E]_0 + K_d + [PL]_0/n - \sqrt{([E]_0 + K_d + [PL]_0/n)^2 - 4[E]_0\,[PL]_0/n}\}/2 \quad (1)$$

where $[PL]_0$, $[E]_0$, and $[E]_b$ are total phospholipid, total enzyme, and bound enzyme concentrations, respectively. This equation assumes that each enzyme binds independently to a site on the interface composed of n phospholipids with dissociation constant K_d.

Monolayer Measurements. Surface pressure (π) of solution in a circular Teflon trough was measured by using a Wilhelmy plate attached to a computer-controlled tensiometer (Nima Technology, Coventry, U.K.). The trough (4 cm diameter × 1 cm deep) has a 0.5-cm deep well for a magnetic stir bar and a small hole drilled at an angle through the wall to allow an addition of protein solution. DHPC solution (5−10 μL in chloroform) was spread onto 10 mL of subphase (10 mM HEPES, pH 7.4, 0.1 M KCl, and 10 mM $CaCl_2$) to form a monolayer with a given initial surface pressure (π_0). The subphase was continuously stirred at 60 rpm with a magnetic stir bar. Once the surface pressure reading of monolayer had been stabilized (after ca. 5 min), the protein solution (typically 50 μL) was injected to the subphase and the change in surface pressure ($\Delta\pi$) was measured as a function of time at 23 °C. Typically, the $\Delta\pi$ value reached a maximum after 20 min. The maximal $\Delta\pi$ value depended on the protein concentration at the low concentration range and reached a saturation when the protein concentration was higher than 2 μg/mL. Protein concentrations were therefore maintained above 4 μg/mL to ensure that the observed $\Delta\pi$ represented a maximal value.

NdeI 1

cat	atg	ggc	ctg	tac	cag	ttc	aaa	aac	atg	atc	cag	tgc	acc
	met	gly	leu	**tyr**	gln	phe	lys	asn	met	ile	gln	cys	thr

10

20

gtt	ccg	tct	cgt	tct	tgg	tgg	gac	ttc	gct	gac	tac	ggt	tgc
val	pro	ser	arg	ser	**trp**	**trp**	asp	phe	ala	asp	tyr	gly	cys

30

40

tac	tgc	ggt	cgt	ggt	ggt	tct	ggt	acc	ccg	gtt	gac	gac	ctg
tyr	cys	gly	arg	gly	gly	ser	gly	thr	pro	val	asp	asp	leu

50

gac	cgt	tgc	tgc	cag	gtt	cac	gac	aac	tgc	tac	aac	gaa	gct
asp	arg	cys	cys	gln	val	his	asp	asn	cys	tyr	asn	glu	ala

60

gaa	aag	atc	tct	ggt	tgt	tgg	ccg	tac	ttc	aaa	acc	tac	tct
glu	lys	ile	ser	gly	cys	**trp**	pro	tyr	**phe**	lys	thr	tyr	ser

70

80

tac	gaa	tgc	tct	cag	ggt	act	ctg	acc	tgc	aaa	ggt	ggt	aac
tyr	glu	cys	ser	gln	gly	thr	leu	thr	cys	lys	gly	gly	asn

90

aac	gca	tgt	gca	gct	gct	gtt	tgc	gat	tgc	gat	cgt	ctg	gct
asn	ala	cys	ala	ala	ala	val	cys	asp	cys	asp	arg	leu	ala

100

110

gca	atc	tgc	ttc	gct	ggt	gct	ccg	tac	aac	aac	aac	aac	tac
ala	ile	cys	phe	ala	gly	ala	pro	tyr	asn	asn	asn	asn	**tyr**

HinDIII

aac	atc	gac	ctg	aaa	gct	cgt	tgc	cag	tag	taa	gct	tcc	acc
asn	ile	asp	leu	lys	ala	arg	cys	gln					

FIGURE 1: Nucleotide sequence of the synthetic *N. n. atra* PLA_2 gene. The sequence is shown in the 5′ to 3′ direction. The amino acid sequence of expressed protein and unique restriction sites are also shown. The mutated amino acids are shown in boldface type. Notice that the amino-terminal Asn is mutated to Gly to facilitate the removal of the initiator Met by Met aminopeptidase. The degenerate DNA sequence of the synthetic gene was inferred from the corrected amino acid sequence based on the preferred codon usage of *E. coli* (*32*).

RESULTS

Expression of Recombinant N. n. atra PLA_2 and Mutants. Two acidic isoforms of PLA_2s, with two substitutions and different activities, have been purified and characterized from the venom of *N. n. atra* (*21*). pMS-nna vector was designed to express the mature form of the more active *N. n. atra* PLA_2 isoform in a T7 promoter-based pET21a vector. As shown in Figure 1, the coding sequence of *N. n. atra* PLA_2 is inserted in frame with initiation codon ATG in the *Nde*I site of pET21a. In *E. coli*, the initiator Met is rapidly removed by methionine aminopeptidase when the next amino acid has a small side chain, such as Gly, Ala, Ser, Cys, Pro, and Thr (*22*). Thus, the amino-terminal Asn of *N. n. atra* PLA_2 was substituted for by Gly. This recombinant protein (N1G) will be referred to as wild type hereafter and all other mutants were prepared using it as a template. Our strategy for the construction of expression vector for *N. n. atra* PLA_2 was similar to that used for the construction of human pancreatic PLA_2 (*16*) and human group V PLA_2 (*17*). When BL21-(DE3) cells harboring pMS-nna were induced by isopropyl β-D-thiogalactopyranoside, *N. n. atra* PLA_2 was expressed as an inclusion body that was sulfonated, solubilized in 5 M guanidinium chloride, refolded, and purified to near homogeneity (>90%). The amino-terminal amino acid sequence analysis of the recombinant protein showed that it is pure *N. n. atra* PLA_2 with the amino-terminal Met fully removed. The overall yield of purified protein was ≈1 mg of protein/L of culture.

We then measured the enzymatic activity of recombinant *N. n. atra* PLA_2 using polymerized mixed liposomes as substrate. The polymerized mixed liposome system allows for separate and accurate measurements of phospholipid headgroup specificity and interfacial preference of PLA_2 (*12*, *13*). The former can be determined by measuring the enzymatic activity toward various inserts in a given polymerized matrix, whereas the latter can be determined by measuring the enzymatic activity toward a given insert in different polymerized matrixes. In this study, zwitterionic pyrene-PE and anionic pyrene-PG were used as hydrolyzable inserts and zwitterionic BLPC and anionic BLPG as polymerized matrixes. The kinetic data (see Table 1) described in terms of second-order rate constant, $(k_{cat}/K_m)^*$ (*5*), show that enzymatic activities of the recombinant *N. n. atra* PLA_2 were lower than those of native protein by ≈30%. Presumably, the Asn-1 to Gly mutation slightly changes the conformation of the amino-terminal α-helix that has been shown to be a part of interfacial binding surface of secretory PLA_2s (*4*, *6*, *23*). The substitution did not, however, appear to affect the catalytic apparatus of the recombinant enzyme as both native and recombinant *N. n. atra* PLA_2 showed the same activity toward monomeric 1,2-dihexanoyl-*sn*-glycero-3-phosphoethanolyamine below its critical micellar concentration (data not shown). Also, both enzymes showed the identical headgroup specificity and interfacial preference; i.e., lack of noticeable phospholipid headgroup specificity and interfacial preference. It is particularly noteworthy that *N. n. atra* PLA_2 has comparable and high activity toward PC and PG membranes, unlike most secretory PLA_2s that significantly prefer anionic membranes to zwitterionic membranes. When compared with human group V PLA_2 that has been shown to be active toward zwitterionic membranes (*7*), the recombinant *N. n. atra* PLA_2 was as active as and 3 times more active than the group V PLA_2 toward pyrene-PE/BLPC and intact human neutrophils, respectively.

Kinetic Properties of N. n. atra PLA_2 Mutants toward Polymerized Mixed Liposomes. The X-ray crystal structure of *N. n. atra* PLA_2 shows that it contains a large number of aromatic residues on its putative interfacial binding surface surrounding the active-site slot (Figure 2). To assess the roles of these aromatic residues in the interfacial catalysis of *N. n. atra* PLA_2, we mutated six aromatic residues in this region to Ala to generate Y3A, W18A, W19A, W61A, F64A, and Y110A. All mutant proteins were expressed, refolded, and purified as described for the wild-type enzyme. Because the side chains of all mutated residues are surface-exposed (Figure 2), their mutations were not expected to have significant effects on the protein structure and stability. Indeed, all mutant proteins were expressed and refolded as efficiently as the wild type (data not shown), except for Y3A, which gave a significantly lower yield (≈0.2 mg of protein/L of culture).

To determine how differently the mutations affect the interfacial catalysis of *N. n. atra* PLA_2, we first measured the activities of wild type and mutants toward various polymerized mixed liposomes (see Table 1). First of all, the mutants showed comparable activities toward pyrene-PE and pyrene-PG, indicating that the mutations have little effect on the headgroup specificity and the interfacial preference of *N. n. atra* PLA_2. In contrast, the effects of the mutations on the overall interfacial activity of *N. n. atra* PLA_2, as

Table 1: Kinetic Properties of *N. n. atra* PLA_2 and Mutants

enzymes	10^5 $(k_{cat}/K_M)_{app}$ (M^{-1} s^{-1}) pyrene-PE/BLPC	pyrene-PG/BLPC	pyrene-PE/BLPG	pyrene-PG/BLPG	relative activity on human neutrophils
native	47 ± 10	45 ± 8	42 ± 7	43 ± 12	1.7
WT[a]	32 ± 3	30 ± 4	32 ± 3	31 ± 3	1.0
Y3A	2.8 ± 0.1	2.5 ± 0.1	2.9 ± 0.1	2.9 ± 0.1	ND[b]
W18A	13 ± 1	16 ± 1	14 ± 1	22 ± 2	0.4
W19A	1.3 ± 0.1	1.5 ± 0.3	1.2 ± 0.2	1.7 ± 0.3	ND
W61A	1.2 ± 0.2	1.4 ± 0.3	1.1 ± 0.1	1.4 ± 0.1	ND
F64A	0.9 ± 0.1	1.1 ± 0.2	1.2 ± 0.3	1.0 ± 0.2	ND
Y110A	4.3 ± 0.3	4.9 ± 0.5	4.8 ± 0.3	5.5 ± 0.2	0.4
hV-PLA_2[c]	31 ± 10	56 ± 10	46 ± 05	75 ± 10	0.3

[a] Recombinant enzyme with N1G mutation. [b] Not detectable. [c] Human group V PLA_2.

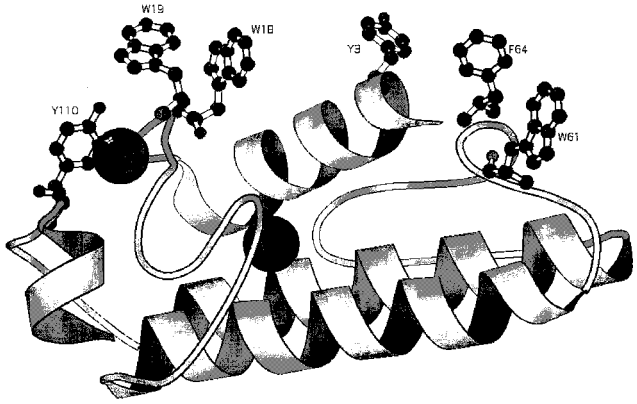

FIGURE 2: Ribbon diagram of *N. n. atra* PLA_2 with mutated aromatic side chains (sticks and balls) and two calcium ions (large black circles). Figure was generated with MOLSCRIPT (*33*). The molecule is oriented with its putative interfacial binding surface pointing upward.

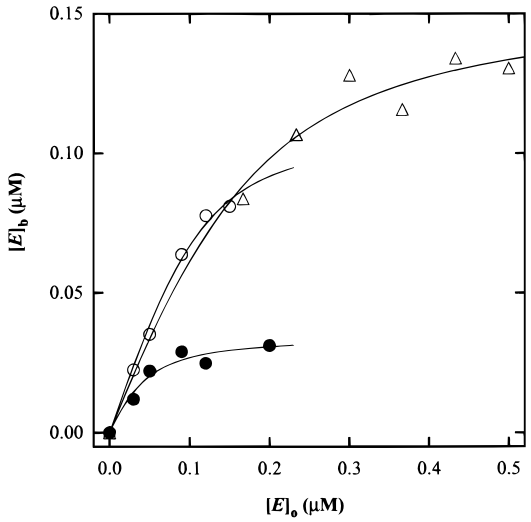

FIGURE 3: Binding of recombinant *N. n. atra* PLA_2 (●), W18A (○), and Y110A (△) selected mutants to DHPC-coated beads. Binding mixtures contained 10 mM Tris-HCl, pH 7.4, 0.16 M NaCl, 1 μM BSA, and 10 mM Ca^{2+}. Bulk DHPC concentration was 200 μM. Data shown here are from one representative measurement for each mutant. Triplicate measurements were made for each mutant for n and K_d determination. The solid lines represent theoretical curves constructed from parameters determined from the nonlinear least-squares fit using eq 1.

indicated by the relative activity of mutants toward various polymerized mixed liposomes, varied to a large degree. W19A, W61A, and F64A were the least active with only about 3% of wild-type activity, followed by Y3A, Y110A, and W18A that retained 10%, 15%, and 40% of the wild-type activity, respectively. The relative activity of mutants to release arachidonate from intact neutrophils compared well with their relative activity toward vesicle substrates. Most notably, W19A, W61A, and F64A showed no detectable activity toward neutrophil membranes for up to 1 h. Taken together, these results suggest that while all the mutated aromatic residues of *N. n. atra* PLA_2 are involved in interfacial catalysis, Trp-19, Trp-61, and Phe-64 make the largest contributions.

Membrane Binding Affinity of N. n. atra PLA_2 Mutants. To understand the origin of the effects of the above mutations on the enzyme activities of *N. n. atra* PLA_2 and to quantitatively assess the contribution of each mutated residue to the energetics of interfacial binding, we measured the binding affinity of wild type and mutants for hydrophobic beads coated with DHPC and DHPG, nonhydrolyzable ether analogues of PC and PG. Phospholipid-coated hydrophobic beads have been shown to be useful in determining the membrane affinity of PLA_2s (*19*). In particular, this model membrane allows rapid and accurate measurement of PC affinity, which normally is difficult to achieve with PC vesicles due to their low pelleting efficiency compared to anionic vesicles. Binding isotherms of wild type and selected mutants for DHPC-coated beads are illustrated in Figures 3 and 4, and n and K_d values determined from curve-fitting to a simple Langmuir-type equation (eq 1) are summarized in Table 2. Note that K_d is expressed in terms of molarity of enzyme binding sites composed of n phospholipids. Thus, nK_d is the dissociation constant in terms of molarity of lipid molecules and the relative binding affinity can be best described in terms of relative values of $(1/nK_d)$.

First of all, wild-type *N. n. atra* PLA_2 showed 3.5-fold higher affinity for PC-coated beads than for PG-coated beads. This modest yet unusual PC preference results from the differences in both n and K_d, suggesting that *N. n. atra* PLA_2 binds PC and PG membranes with different affinities and in different modes. It appears that *N. n. atra* PLA_2 binds to anionic PG beads with about 13-fold lower affinity (i.e., higher K_d) but can be more compactly adsorbed to the lipid surfaces (i.e., lower n). The origin of this difference is not clear at present. In general, the mutations affect both n and K_d values, albeit to different degrees, suggesting that they have effects on both binding affinity and binding mode. Most importantly, the overall relative binding affinity of mutants correlates well with their relative activity toward polymerized mixed liposomes, indicating that the reduced interfacial activities of these mutants are largely due to their reduced interfacial binding affinities. This in turn indicates that the

Table 2: Membrane Binding Affinity of *N. n. atra* PLA_2 and Mutants[a]

	DHPC beads					DHPG beads			
enzyme	n	K_d (μM)	nK_d (μM)	relative affinity	$\Delta\Delta G°/\Delta A$ (cal mol^{-1} Å^2)	n	K_d (μM)	nK_d (μM)	relative affinity
WT	170 ± 20	0.02 ± 0.01	3.4 ± 2.0	1.00		48 ± 7	0.27 ± 0.03	13 ± 2	1.00
W18A	540 ± 45	0.02 ± 0.01	11 ± 5	0.32	5	89 ± 9	0.26 ± 0.01	23 ± 2	0.56
W19A	470 ± 80	0.45 ± 0.05	212 ± 43	0.02	18	78 ± 13	1.10 ± 0.20	81 ± 20	0.16
W61A	210 ± 30	0.64 ± 0.11	134 ± 30	0.03	16	130 ± 18	0.74 ± 0.16	96 ± 24	0.14
F64A	160 ± 19	0.76 ± 0.17	122 ± 30	0.03	22	150 ± 11	0.75 ± 0.13	113 ± 20	0.12
Y110A	380 ± 28	0.06 ± 0.01	23 ± 4	0.15	13	110 ± 15	0.42 ± 0.01	46 ± 6	0.28

[a] Y3A was not included because of the insufficient amount of the protein for these measurements.

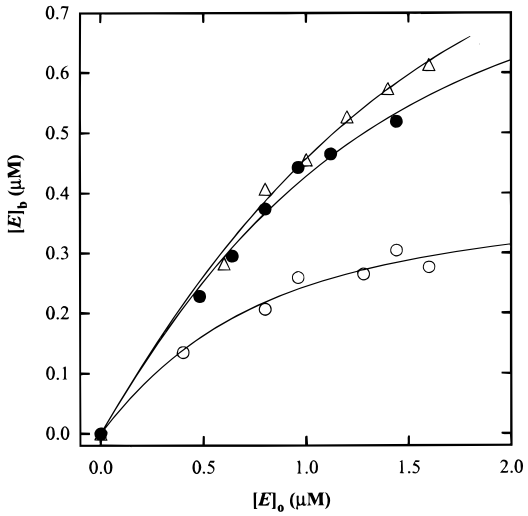

FIGURE 4: Binding of recombinant W19A (●), W61A (○), and F64A (△) selected mutants to DHPC-coated beads. Experimental conditions were the same as described for Figure 3 except that bulk DHPC concentration was 300 μM.

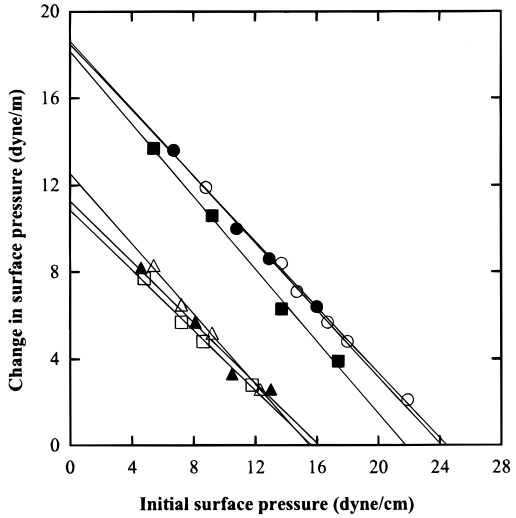

FIGURE 5: Penetration of *N. n. atra* PLA_2 and mutants to DHPC monolayers. Proteins include wild type (○), W18A (●), W19A (△), W61A (▲), F64A (□), and Y110A (■). The subphase contained 10 mM HEPES buffer, pH 7.4, 10 mM Ca^{2+}, and 4 μg/mL of each protein. Each data point represents an average from duplicate measurements.

surface aromatic residues of *N. n. atra* PLA_2, Trp-19, Trp-64 and Phe-61 in particular, play essential roles in the interfacial binding of this active enzyme. With anionic DHPG-coated beads, the mutations had 2−8 times smaller effects on binding affinity than observed with DHPC-coated beads. This again suggests that *N. n. atra* PLA_2 might bind to anionic membranes in a slightly different mode in which the interactions between the aromatic side chains and membrane phospholipids are suboptimal.

Monolayer Penetration of N. n. atra PLA_2 Mutants. To better understand the differential effects of the mutations of surface aromatic residues on the interfacial binding of *N. n. atra* PLA_2, we measured the penetration of wild type and mutants into the DHPC monolayer at the air−water interface. In these studies, a phospholipid monolayer of a given initial surface pressure (π_0) was spread at constant area and the change in surface pressure ($\Delta\pi$) was monitored after injection of protein into the subphase. Figure 5 shows that the three mutants with the lowest interfacial affinity (W19A, W61A, and F64A) penetrate into DHPC monolayers significantly less effectively than wild type over a wide range of π_0. The monolayer penetration ability of the three mutants was similar to that of human group IIa PLA_2 that has extremely low activity on PC monolayers and bilayers. In contrast, W18A and Y110A showed similar and modestly lower monolayer penetrating power, respectively, when compared to the wild type. These data thus suggest, albeit qualitatively, that essential roles of Trp-19, Trp-61, and Phe-64 in interfacial binding derive from their ability to penetrate into zwitterionic PC membranes, thereby making favorable interactions with phospholipids.

DISCUSSION

It has been long known that cobra venom has high hemolytic activity, which has been attributed mainly to its PLA_2 activities. Cobra venom PLA_2s, most notably acidic PLA_2s from *Naja naja naja* and *N. n. atra*, have high activities on condensed PC vesicles and intact mammalian cell membranes. Earlier studies showed that these enzymes have higher membrane penetration power than other secretory PLA_2s (*24*). However, the molecular mechanisms underlying these unusual activities have not been fully elucidated. The interfacial catalysis of PLA_2s involves interfacial binding prior to the catalytic steps. Both electrostatic and nonelectrostatic forces are involved in the interfacial binding of PLA_2 (*8*). For many secretory PLA_2s that favor anionic membranes, interfacial binding is in large part driven by Coulombic interactions between cationic interfacial binding residues of protein and anionic membrane surfaces (*3*−*6*). For cytosolic PLA_2 (*20*) and other secretory PLA_2s with relatively high activity on zwitterionic membranes (*7*, *25*), non-Coulombic interactions, including hydrophobic interactions, play more important roles. Results described herein demonstrate that the high activities of *N. n. atra* PLA_2 toward PC vesicles and intact cell membranes derive mainly from non-Coulombic interactions between aromatic side chains on its putative

interfacial binding surface and zwitterionic membrane surfaces. *N. n. atra* PLA_2 has a single cationic residue, Lys-6, on the interfacial binding surface and consequently shows no preference for anionic membranes. In fact, *N. n. atra* PLA_2 binds PC-coated beads 3 times more tightly than PG-coated beads. Differences in both n and K_d values indicate that *N. n. atra* PLA_2 binds the two membranes with different affinities and orientations. Nevertheless, *N. n. atra* PLA_2 showed the same activity toward BLPC and BLPG polymerized mixed liposomes (see Table 1) because essentially all enzymes molecules are fully bound to liposomes under our kinetic conditions (*6*).

Among six aromatic residues located on the putative interfacial binding surface of *N. n. atra* PLA_2, the mutations of three residues, Trp-19, Trp-61, and Phe-64, show the largest effects (up to 50-fold decrease) on its enzymatic activities and membrane-binding affinities. Good correlation between the relative enzymatic activity and relative membrane affinity of mutants indicates that these essential residues are mainly involved in interfacial binding but not in catalysis per se. It appears that Tyr-3 and Tyr-110 make lesser yet significant contributions to interfacial binding. Presumably, they make less intimate contact with membranes due to their locations and side-chain orientations. Finally, Trp-18 does not appear to be directly involved in interfacial binding. This finding is consistent with our previous study on bovine pancreatic PLA_2 showing that a residue (i.e., Leu) at position 18 interacts mainly with the acyl chain of the active-site bound phospholipid, but not with membrane surfaces, because of its side-chain orientation (*26*). Also, an NMR study of *N. n. naja* PLA_2 points to the involvement of Trp-18 in substrate interactions (*27*).

Our monolayer data suggest that Trp-19, Trp-61, and Phe-64, but not Trp-18 and Tyr-110, are involved in membrane penetration. However, these measurements could not quantitatively determine the degree of penetration by each amino acid. We have previously reported a simple thermodynamic calculation to estimate the degree of membrane penetration for each amino acid (*20*). In this method, the change in free energy of binding per change in accessible surface area caused by each mutation ($\Delta\Delta G°/\Delta A$) is calculated and compared with the $\Delta\Delta G°/\Delta A$ value for transferring amino acids and alkanes from ethanol to water (ca. 24 cal mol^{-1} $Å^{-2}$) (*28*). As summarized in Table 2, $\Delta\Delta G°/\Delta A$ is the highest for F64A (22 cal mol^{-1} $Å^{-2}$), indicating that Phe-64 is essentially fully inserted into the membrane during the interfacial binding of *N. n. atra* PLA_2. On the other hand, the mutations of Trp-19 and Trp-61 give smaller and comparable $\Delta\Delta G°/\Delta A$ values (16−18 cal mol^{-1} $Å^{-2}$), indicating that they are partially inserted into the membrane. It has been shown for transmembrane proteins that Trp and Tyr are enriched near the ends of the transmembrane helices whereas Phe is more frequently found in the core of the helices (*29*, *30*). Also, Trp is shown to have high propensity for the lipid−water interface (*31*). Therefore, it appear that the side chains of Phe-64 and the two tryptophans interact with membranes in distinctive mode because of the difference in their intrinsic membrane propensity. However, the fact that Trp-19, Trp-61, and Phe-64 are equally important for the interfacial binding of *N. n. atra* PLA_2 indicates that both binding modes are equally effective in enhancing the interfacial binding affinity. In summary, this structure−function study of *N. n. atra* PLA_2 shows that all aromatic residues, Trp, Tyr, and Phe, can play important roles in interfacial binding, especially binding to zwitterionic membranes, and that their relative contribution depends on the chemical nature, the location, and the orientation of side chains.

ACKNOWLEDGMENT

We thank Kwang Pyo Kim for helping us with cell studies.

REFERENCES

1. Dennis, E. A. (1997) *Trends Biochem. Sci. 22*, 1−2.
2. Scott, D. L., and Sigler, P. B. (1994) *Adv. Protein Chem. 45*, 53−88.
3. Dua, R., Wu, S.-K., and Cho, W. (1995) *J. Biol. Chem. 270*, 263−268.
4. Han, S.-K., Yoon, E. T., Scott, D. L., Sigler, P. B., and Cho, W. (1997) *J. Biol. Chem. 272*, 3573−3582.
5. Snitko, Y., Koduri, R., Han, S.-K., Othman, R., Baker, S. F., Molini, B. J., Wilton, D. C., Gelb, M. H., and Cho, W. (1997) *Biochemistry 36*, 14325−14333.
6. Snitko, Y., Han, S. K., Lee, B. I., and Cho, W. (1999) *Biochemistry 38*, 7803−7810.
7. Han, S. K., Kim, K. P., Koduri, R., Bittova, L., Munoz, N. M., Leff, A. R., Wilton, D. C., Gelb, M. H., and Cho, W. (1999) *J. Biol. Chem. 274*, 11881−11888.
8. Gelb, M. A., Cho, W., and Wilton, D. C. (1999) *Curr. Opin. Struct. Biol. 9*, 428−432.
9. Baker, S. F., Othman, R., and Wilton, D. C. (1998) *Biochemistry 37*, 13203−13211.
10. White, S. T., Scott, D. L., Otwinowski, Z., Gelb, M. H., and Sigler, P. B. (1990) *Science 250*, 1560−1563.
11. Comfurius, P., and Zwaal, R. F. A. (1977) *Biochim. Biophys. Acta 488*, 36−42.
12. Wu, S.-K., and Cho, W. (1993) *Biochemistry 32*, 13902−13908.
13. Wu, S.-K., and Cho, W. (1994) *Anal. Biochem. 221*, 152−159.
14. Kates, M. (1986) *Techniques of Lipidology*, 2nd ed., Elsevier, Amsterdam.
15. Thannhauser, T. W., Konishi, Y., and Scheraga, H. A. (1984) *Anal. Biochem. 138*, 181−188.
16. Han, S.-K., Lee, B.-I., and Cho, W. (1997) *Biochim. Biophys. Acta 1346*, 185−192.
17. Han, S.-K., Yoon, E. T., and Cho, W. (1998) *Biochem. J. 331*, 353−357.
18. Maraganore, J. M., Merutka, G., Cho, W., Welches, W., Kézdy, F. J., and Heinrikson, R. L. (1984) *J. Biol. Chem. 259*, 13839−13843.
19. Kim, Y., Lichtenbergova, L., Snitko, Y., and Cho, W. (1997) *Anal. Biochem. 250*, 109−116.
20. Bittova, L., Sumandea, M., and Cho, W. (1999) *J. Biol. Chem. 274*, 9665−9672.
21. Pan, F. M., Chao, S. C., Wu, S. H., Chang, W. C., and Chiou, S. H. (1998) *Biochem. Biophys. Res. Commun. 250*, 154−160.
22. Hirel, P. H., Schmitter, M. J., Dessen, P., Fayat, G., and Blanquet, S. (1989) *Proc. Natl. Acad. Sci. U.S.A. 86*, 8247−8251.
23. Liu, X., Zhu, H., Huang, B., Rogers, J., Yu, B. Z., Kumar, A., Jain, M. K., Sundaralingam, M., and Tsai, M. D. (1995) *Biochemistry 34*, 7322−7334.
24. Demel, R. A., Geurts van Kessel, W. S. M., Zwaal, R. F. A., Roelofsen, B., and van Deenen, L. L. M. (1975) *Biochim. Biophys. Acta 406*, 97−107.
25. Ghomashchi, F., Lin, Y., Hixon, M. S., Yu, B. Z., Annand, R., Jain, M. K., and Gelb, M. H. (1998) *Biochemistry 37*, 6697−6710.
26. Lee, B.-I., Yoon, E. T., and Cho, W. (1996) *Biochemistry 35*, 4231−4240.

27. Plesniak, L. A., Yu, L., and Dennis, E. A. (1995) *Biochemistry 34*, 4943−4951.
28. Chothia, C. (1974) *Nature 248*, 338−339.
29. Wallin, E., Tsukihara, T., Yoshikawa, S., von Heijne, G., and Elofsson, A. (1997) *Protein Sci. 6*, 808−815.
30. Braun, P., and von Heijne, G. (1999) *Biochemistry 38*, 9778−9782.
31. Yau, W. M., Wimley, W. C., Gawrisch, K., and White, S. H. (1998) *Biochemistry 37*, 14713−14718.
32. deBoer, H. A., and Kastelein, R. A. (1986) in *Maximizing Gene Expression* (Reznikoff, W., and Gold, L., Eds.) pp 225−235, Butterworths, Boston, MA.
33. Kraulis, P. J. (1991) *J. Appl. Crystallogr. 24*, 946−950.

BI9921384